Defining Allowable Stimulus Ranges for Position and Force Controlled Cutaneous Cues

Janelle P. Clark, *Member, IEEE,*[1] and Marcia K. O'Malley, *Fellow, IEEE*[2]

***Abstract*—Haptic cues delivered via wearable devices have great potential to enhance a user's experience by transmitting task information and touch sensations in domains such as virtual reality, teleoperation, and prosthetics. Much is still unknown on how haptic perception, and consequently optimal haptic cue design, varies between individuals. In this work we present three contributions. First, we propose a new metric, the Allowable Stimulus Range (ASR), as a way to capture subject-specific magnitudes for a given cue, using the method of adjustments and the staircase method. Second, we present a modular, grounded, 2-DOF, haptic testbed designed to conduct psychophysical experiments in multiple control schemes and with rapidly-interchangeable haptic interfaces. Third, we demonstrate an application of the testbed and our ASR metric, together with just noticeable differences (JND) measurements, to compare perception of haptic cues delivered via position or force control schemes. Our findings show that users demonstrate higher perceptual resolution in the position-control case, though survey results suggest that force-controlled haptic cues are more comfortable. The results of this work outline a framework to define perceptible and comfortable cue magnitudes for an individual, providing the groundwork to understand haptic variability, and compare the effectiveness of different types of haptic cues.**

***Index Terms*—tactile perception, haptic feedback, wearable devices, psychophysics, discrimination, detection, skin stretch, indentation, normal cues, tangential cues, position control, force control**

I. Introduction

Wearable haptic devices are becoming increasingly common as we seek new means of transferring information between people and technology. While vibration is a ubiquitous cutaneous haptic cue, devices that convey normal and shear forces are increasingly common, since these modalities are well-suited to convey continuous rather than discrete information to users. Some example applications requiring continuous information that integrates haptic feedback via normal and shear forces include an amputee regaining a sense of touch [1], [2], enabling a robot operator to complete distant dexterous tasks [3], or adding realism when navigating a virtual environment [4]. In each scenario, the purpose of the haptic feedback is to provide the user with time-varying position or force cues that map to the actions of the user as they interact with the environment. Even in cases where the feedback is inadvertent and uncomfortable, it is a desirable asset [5]. It is important to understand how the user's tactile acuity, or sharpness in sensing the stimuli [6], might impact the effectiveness of the wearable haptic system to support these tasks.

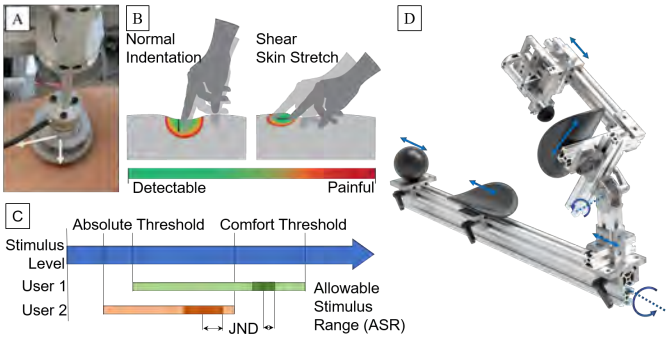

Fig. 1. A cutaneous haptic cue testbed for quantifying the Allowable Stimulus Range (ASR). A) The testbed end effector can apply normal indentation and shear stretch cues to the arm in either position- or force-control modes. B) We seek to quantify the range of allowable cue amplitudes, from just detectable to comfort limits, below pain thresholds in both normal and shear directions. C) The Allowable Stimulus Range (ASR) is unique to an individual, and is defined by the absolute threshold (minimum) to the comfort threshold (maximum). The Just Noticeable Difference is contained with the ASR. D) The testbed can be configured to apply cues to different upper limb locations.

To demonstrate the effectiveness of a wearable haptic device, we must consider not only the mechanical capabilities of the device but also the user's tactile acuity. Researchers typically report the results of experiments covering at least one of three performance assessment categories: quantifying or characterizing the mechanical specifications of the device, assessing a user's ability to perceive a haptic cue generated by the device, or determining the user's rating of the physical experience provided by the device and cue. Characterization tests quantify achievable haptic cue magnitudes and repeatability of cue generation [7]–[9]. Haptic perception experimental studies aim to evaluate human perception of the cues generated by wearable haptic devices, with subjects responding to prompts that are intended to quantify what they feel, either by measuring the accuracy of cue identification or, through psychophysical experiments, measuring the detection of cues or the discriminability of cues that vary in one or more features [10]–[15]. Qualitative assessments address ergonomic, affective, and illusionary feedback and ratings, i.e. the degree to which the haptic cue has the desired effect, if it is pleasant, or if the cue feels continuous [8], [11], [16], [17].

These types of assessments are typically administered independently, emphasizing the capabilities of the device or

This work was supported by the National Science Foundation, Grant 2127309 to the Computing Research Association for the CIFellows 2021 Project. This was also supported by NSF grant CMMI-1830146.

[1]Department of Computer Science, University of Massachusetts Lowell, Lowell, MA, 01851

[2]Department of Mechanical Engineering, Rice University, Houston, TX, 77251

Corresponding Author: janelle_clark@uml.edu

the user's perception of the cues and separately assessing the user's comfort in one of two ways. The first is through surveys and verbal feedback after the experiment takes place [18]–[22]. The second is to run pilot experiments to determine cue ranges deemed safe to be unilaterally applied to all users [8], [16], [22]–[25]. This technique is not necessarily effective since pilots use a smaller number of subjects, with one study highlighting that some participants even feared the discomfort from the device [26]. There are a few device studies that incorporate assessments of both user perception and comfort. Several previous studies personalize the haptic cues to be within perceptible and comfortable ranges for the users; however, the ranges are not reported, as the studies focus on discrimination accuracy for various haptic cues [27]–[29]. One study reports comfort thresholds for individual subjects, showing the maximum comfortable squeeze force on the wrist [30]. While haptic devices typically rely on the stimulation of mechanoreceptors in the skin, at some magnitude any stimulus may also induce responses from nociceptors, which reflect pain [31]. To avoid this scenario, an upper bound for a stimulus should be determined to be integrated into our definition of the haptic cue design space for an individual. We expect this design space, which defines the range of parameters that are appropriate for a given user, to be unique for each haptic modality (e.g. normal indentation and shear skin stretch).

A. Background

In this paper, we focus on the perception of two modalities of cutaneous haptic cues that are typically rendered with wearable haptic devices, namely skin stretch and normal indentation (Fig. 1b). Depending on the mechanism of actuation, cues are rendered to the skin using either position or force control techniques.

1) Haptic Modalities: Skin stretch describes the production of shear forces on the skin, and skin stretch haptic devices are designed to create tangential forces as the primary mode of haptic feedback to the user. The actuation design for wearable skin stretch devices can vary, most commonly with rockers rotating on the arm [9], [13], [32]–[34], lateral pulls on pads adhered to the skin [16], [17], [35], [36], or by laterally moving an indentor [7], [14], [15], [26], [37]. Other examples include bands that twist the arm or pull back and forth [22], [38].

Indentation describes a force applied to the arm, normal to the skin surface, in a discrete location [7], [8], [10], [11], [26], [26], [39]–[42]. It is also possible to apply normal forces radially around the entire arm at once, typically referred to as squeeze [12], [30], [43]–[45], though for this paper we are specifically interested in discrete, localized indentation.

2) Control Schemes: Position control is the most common control scheme used to generate haptic cues, due to the widespread use of low-cost, compact, low-power, and lightweight servo motors in wearables. When servos are not practical, miniature DC motors and encoders for position sensing are a common alternative [9], [13]–[16], [26], [32], [36], [37], [39], [43], [45]–[47]. When haptic cues are delivered in a position control scheme, the forces applied to the skin are the result of the causal relationship between skin displacement and force. The relationship between the commanded displacement of the device on the skin and the haptic experience of the user is often described in the context of the corresponding force, but without direct force measurements.

There is some evidence that the use of position control to generate repeatable haptic cues, though convenient due to widely available hardware components that facilitate position control, could be contributing to the heterogeneity of haptic experiences by users. The nonlinearity of skin properties is a known phenomenon that can lead to irregular force responses to similar skin displacements. To address this, some researchers have developed mappings [23], [42], [48]. Mappings are a nonlinear conversion between the information that the designer is trying to convey to the user and the haptic cue parameters that are used to generate the cue perceived by the user. For example, if skin stretch is being used to indicate the closure of a robotic gripper, a designer might choose a sigmoid mapping, where one degree of closure from an open gripper would result in more skin stretch from the device than one degree of closure when the gripper is almost closed.

A force control approach to regulating the delivery of haptic cues would serve as an alternative to such mappings. In this scenario, a target force would be applied to the skin regardless of the linearity of the skin's material properties, or of an individual's physiology. Among the wearable haptic devices that we surveyed for this paper, only five feature closed-loop force control [19], [25], [30], [49], [50]. This is not surprising, since closed-loop force control requires the integration of force sensors, which are typically more expensive than position sensors. We hypothesize that cues that are delivered with the interaction forces being controlled (rather than the degree of skin deflection being controlled) may provide a means for ensuring consistent perception of haptic cues across subjects who may exhibit different tactile perception acuity. In this paper, we present results for experiments conducted in both position and force control modes to test this hypothesis. To date, detailed analyses of the perception of cues generated via force control as compared to those generated via position control has not been presented in the literature.

B. Contributions

In this work, we present three main contributions. First, we define the *allowable stimulus range* (ASR) and present a method for its determination. The ASR provides a holistic picture of a user's tactile acuity for a given haptic cue, and our results define ASR for four cues using a series of psychophysical tests (two modalities, normal skin indentation and skin stretch, and two control schemes, position and force control). Position control has been the typical method for precise haptic cue delivery, though force control is also of interest for display of haptic cues. Second, in order to complete these assessments, we introduce a new haptic test bed for precise delivery of tangential skin stretch and normal indentation cues to the arm that can be delivered via closed-loop position or force control operation modes. Third, the characteristics of the ASR under the two control schemes are compared in order to determine what benefit, if any, exists in using one control scheme over another to deliver cutaneous haptic cues to the arm.

II. Allowable Stimulus Range

We present a new measure of an individual user's haptic acuity, the *allowable stimulus range* (ASR), which is determined based on the results of standard psychophysical assessments. The ASR describes the range of detectable and comfortable values for any sensory parameter for a given individual, and is reported in the same units as the stimulus. The ASR is unique to each individual, and provides haptic device designers with a clear picture of the tactile acuity of an individual for perceiving haptic cues. Two thresholds are measured to characterize an individual's ASR and the haptic perceptual resolution that can be achieved with a haptic device. The ASR is bounded by the absolute threshold at the low end, and the maximum comfort threshold at the high end. These are defined as the minimum detectable cue and the maximum cue strength that is comfortably perceived, respectively (Fig. 1c). The ASR provides the span of allowable cue magnitudes for an individual, and complements the measure for perceptual resolution, the just noticeable difference (JND) threshold, indicating how much a cue needs to change to be differentiated from a given reference value [51].

The ASR provides a clear picture of an individual's tactile acuity. If they have a narrow ASR and a large JND, then there may be a limited number of cues that can be generated by the utilized haptic device that the individual would be able to reliably differentiate. As such, that particular haptic cue may only be suitable for notifications or other binary or state information. For applications requiring the transmission of more detailed information encoded as haptic cues, we would desire that subjects show wide ASRs and small JNDs, indicating they can reliably detect small changes in the stimulus, providing a larger number of distinguishable cues for transmission of more detailed and nuanced information to the user.

We expect that by quantifying the ASR for different haptic modalities and control modes, we will demonstrate the extent to which a particular cue type and implementation may result in generalized haptic experiences for a range of users. The results also allow us to compare the JND for normal indentation and skin stretch under both position and force control modes, normalized by their respective ASRs, to ascertain any advantage in using one control mode over the other.

III. Hardware Design

A high-fidelity haptic test bed was designed to deliver precisely controlled skin stretch and indentation haptic cues to the arm. The test bed features high resolution position and force sensors that are needed for precise closed-loop control of haptic cue delivery, as well as to facilitate quantitative analyses of a wide range of outcome metrics related to haptic cue delivery and human perception (Fig. 1d).

A grounded test bed, rather than a wearable system, was chosen to ensure accurate delivery and sensing of cues. Grounded devices are set on a static, grounded plane, such as a table or floor, with reference planes independent of the participant's movements, whereas wearable devices are those mounted on the body. Though the ultimate motivation for the studies presented in this paper is to inform the design of salient haptic cues that can be delivered via *wearable* devices, it is common for devices to have a grounded counterpart or test bed equivalent that allows for isolation of the cue when testing cue characteristics and human perception [20], [46], [48], [52]. A grounded test bed provides an opportunity to further isolate the cue behavior from sources of noise associated with straps and other attachment points of wearables and allow for the integration of more precise actuators and sensing equipment than is achievable in a wearable form factor.

The mechanical subsystem of the experimental test bed for skin stretch and indentation cues consists of several components. The haptic module is actuated by a 2 degree of freedom (DOF) control unit used to control displacement of the end-effector in two directions, one normal to the surface of the skin, and one tangential to the skin's surface (Fig. 1a). The hemispherical end-effector is the component in contact with the skin. The test bed features a fully adjustable arm rest to achieve a comfortable and natural resting position for the participant during experimentation. Other subsystems include the electrical control unit and the user interface.

A. Mechanical Subsystem

1) Haptic Module Design: A capstan transmission design is employed in the haptic module to achieve smooth linear motion without backlash. A threaded spool is mounted on the motor shaft with the cable wound around it such that, as the motor spins, the spool progresses along the cable length. The DOF for normal and shear motion are actuated with two motors mounted to the carriage of 80 mm Nippon SEBS 7WB linear rails (Fig. 2). The linear rails for the two DOFs are mounted perpendicularly on a square base. The module is fixed to the arm rest at the carriage controlling the normal direction, and the shear carriage holds the end-effector of the haptic interface.

The linear rails provide a 48.8 mm (1.92 in) stroke for each DOF, which is more than sufficient for the normal and shear displacements evaluated in this paper. The haptic module is actuated with two Maxon DCX14L 12V motors with a GPX14 LZ 35:1 gearbox. The motor provides up to 200 mNm of nominal torque, or 47.4 N of lateral force, well able to provide the loads elicited in previous work of 10 N [45], [53]. Position sensing with an ENX10 EASY encoder provides 1024 counts per motor revolution, in combination with the gearbox resulting in a final sensing resolution of 35,840 counts per output shaft revolution. The spool consists of an adapted 3/8 - 16 threaded rod, with a pitch diameter of 8.84 mm (0.348 in) attached to the motor shaft with a set screw.

2) Haptic Interface End-Effector: The haptic interface end-effector is the component in direct contact with the skin, producing the haptic cue. The end-effector consists of a 28mm diameter plastic hemisphere 3D printed with Prusa PLA filament, screwed onto a permanently attached intermediate disk of the same material with a threaded rod for easy installation. It is attached at the center plane to an ATI Nano-17 6-axis force-torque sensor to measure the skin-interface force interactions (Fig. 2). The force sensor resolution is 1/320 N for forces in each xyz direction and 1/64 mNm for torques about each

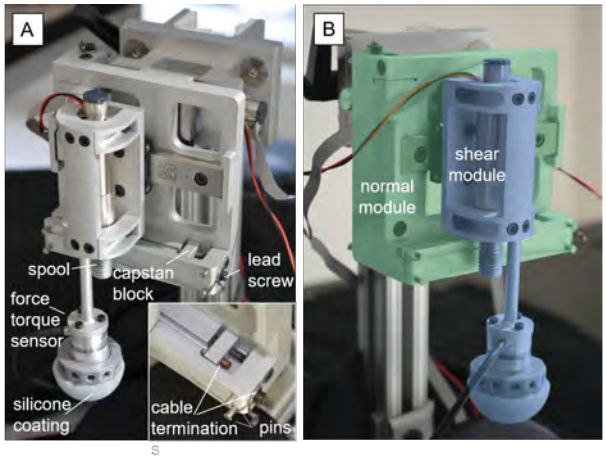

Fig. 2. The two actuation modules consist of A) two independent linear capstans mounted perpendicularly on a square base to create normal (green) and shear (blue) haptic cues. B) The linear capstan assembly includes a linear capstan and a force-torque sensor with a silicone interface.

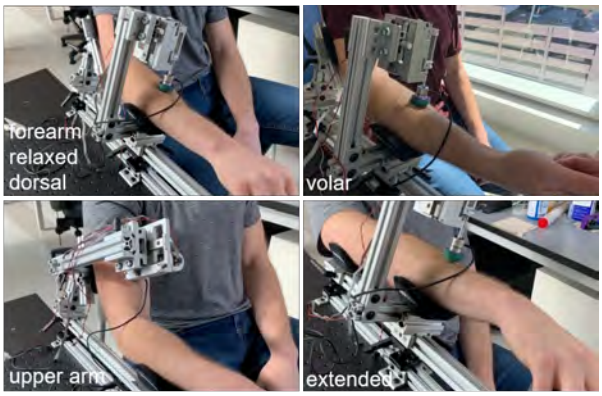

Fig. 3. The modular and adjustable arm rest can be used to test the forearm or upper arm in an extended or relaxed posture. The forearm can be tested on the volar or dorsal side.

xyz axis, as reported by the manufacturer. The end-effector diameter and material is chosen to be comparable to previous works and to be similar to other wearable haptic interfaces [23], [53]. The surface of the haptic interface end-effector is coated with a 1 mm layer of Ecoflex 00-50 silicone to increase traction of the haptic interface. A custom mold, also 3D printed, was made to hold the end-effector in the mold to create the silicone layer, which was then adhered to the end-effector using Loctite 401 adhesive and Loctite SF770 primer. The material and manufacturing choices for this test bed also allow for complex end-effector designs and rapid prototyping, providing the ability to test many shapes and sizes.

The haptic assembly is mounted to the linear carriage for shear displacements with a custom bracket leaving 48.6 mm (1.91 in) of clearance between the end-effector surface and the bottom of the haptic module to ensure the haptic interface and the arm rests are the only points of contact with the arm.

3) Arm Rest Design: The haptic module is grounded to a custom arm rest, designed to be fully adjustable to accommodate a relaxed posture for the subject (Fig. 1d). The use of 1-inch t-slotted framing results in sturdy construction and flexible configurations for applying haptic cues to different areas of the arm. The base bar is mounted to a mechanical breadboard, which is attached to the forearm bar with two locking hinges allowing for a comfortable shoulder abduction angle. The height of the forearm bar is adjustable through the experiment table, an Uplift V2 commercial standing desk.

The upper arm rest has two DOFs, to adjust the height and the shoulder flexion angle, and attaches to the forearm bar by a locking 1-inch, flanged bearing carriage. On the forearm and upper-arm bars are two Profile Designs Ergo Injected arm rests The dimensions of the arm rest are designed to accommodate arm sizes up to the ninetieth percentile in men and down to the tenth percentile in women [54].

The arm rest is designed to allow multiple testing configurations (Fig. 3). The haptic module can be mounted for testing on either the forearm or upper arm. Testing can be done on the dorsal or volar side of the forearm through the choice of two handle options, a 1.4 in (35.56 mm) ball to rest the hand on for testing the dorsal side or a 2 in (50.8 mm) trough to place the hand in palm-side up for testing the volar side. For each of the three configurations, the user can be positioned with the arm relaxed, as described above, or the upper-arm assembly can be removed and the table height increased so that the arm is fully extended. There are other possible configurations available, for example by adjusting the orientation of the bar for the haptic module, demonstrating the advantages of the modular and easily customizeable design.

B. Motor Driver Electronics Subsystem

The motors that actuate the end-effector are controlled using an Escon Module 24/2 Servo Controller mounted to a custom designed circuit-board and a Power Electronics 18V MB120 medical grade power supply. The DAQ interface is a Quanser Q8-USB, handling the force-torque sensor, encoder, and motor controller outputs and the motor command input.

C. User Input Interface Subsystem

An Xbox adaptive controller was selected as the interface for acquiring user responses during psychophysical experiments. The adaptive controller features two large buttons and arrow buttons to capture user responses to prompts displayed on a screen during experimentation.

D. Controller Design

The normal and shear cues provided to the skin are realized through control of the two actuation modules in either a position control or force control mode. In the position control case, the end-effector is commanded to displace a prescribed amount. In the force control case, the interaction force (either normal or shear) is prescribed. The same controllers are used for each independently controlled actuation module.

1) Position Control: Position control is implemented using a standard proportional-derivative (PD) controller

$$\tau = k_p(x_d - x) + k_d(\dot{x}_d - \dot{x}) \quad (1)$$

where x and $\dot{x}$ represent the measured position and velocity, and x_d and $\dot{x}_d$ represent the desired position and velocity. We used a k_p value of 500e-6 kN and a k_d value of 10e-6 kNs.

2) Force Control: The force controller implementation is similar to that of the position-based PD controller. In this case, the proportional term of the controller is dependent on the difference between the measured force and the desired force. For the derivative term, instead of computing the derivative of force error, we use the difference between the desired and measured velocity of the end-effector. A similar approach was implemented in the force control of Tasbi, a wearable haptic device for the wrist [30]. This approach was used for the test bed force control implementation because a traditional PD type force controller was not able to be tuned to a stable configuration for the required bandwidth using the force time-derivative. With the motors active, the force measurements became very noisy. This could be exacerbated by the position of the force sensor at the end of the long cantilever (Fig. 2).

The force and velocity error terms are computed either along the x or z axes depending on the DOF being controlled. These error terms are multiplied by the gains to calculate the commanded motor torque, τ, specifically k_p, 4000e-6 m, and k_d, 150e-6 kNs, calculated as

$$\tau = k_p(f_d - f) + k_d(\dot{x}_d - \dot{x}) \tag{2}$$

where f and f_d represent the measured and desired force values $\dot{x}$ and $\dot{x}_d$ represent the current and desired linear velocity values of the end effector.

IV. Methods

We conducted a series of experiments using our haptic test bed to define the Allowable Stimulus Range (ASR) and just noticeable difference in cue amplitude for two types of haptic cues (normal indentation and shear skin stretch) under two different control schemes (force and position control). The ASR upper and lower bounds for both position and force were defined for each subject using a position control scheme and are reported in units of displacement or force depending on the scheme. We also determined the JNDs for each cue type under both position and force control schemes.

A. Participants

Sixteen able-bodied subjects (age 23.3 ± 3.3 years, 6 female, 1 left handed) completed the experiment. The participants did not claim any physical or cognitive impairment that could interfere with their ability to follow the instructions of the study, nor any pathology that could affect tactile sensation or muscular activity of the forearm. The methods and procedures described in this paper were carried out in accordance with the recommendations of the Institutional Review Board of Rice University (IRB-FY2019-49) with written informed consent obtained from all participants.

B. Experimental Conditions

We conducted three psychophysical experiment types distributed over three, one-hour sessions. In Session 1, the maximum thresholds were measured to define the maximum comfort value of displacement of the end-effector against the skin, and the minimum thresholds were found. Both sets of thresholds were determined using the test bed in a position control scheme. Sessions 2 and 3 consisted of JND assessments in order to find the normal and shear thresholds under both position and force control schemes. The order of presentation of control scheme was randomized, such that a single control scheme was used within a session. Within a session, JNDs were determined for both normal indentation and shear cues. The resulting four conditions were position-normal, position-shear, force-normal, and force-shear.

Fig. 4. The user is seated in front of a monitor with their right arm in the test bed, adjusted according to their comfort. Headphones playing pink noise mask any audible noise from the test bed's motors. The user interface sits either on the table in front of them or on their lap, according to their preference.

C. Experimental Set-Up

The test bed was placed on an adjustable height table to the right of the subject. The subject was seated in a chair in front of a desk with a monitor (Fig. 4). The monitor provides experimental protocol information and prompts, and the user provides their responses through the user interface, kept on the desk in front of them or on their lap. The user interface has two buttons corresponding to two blocks on the screen, lighting up with the associated stimuli actuation during a trial. The participant can also use a set of arrow keys for the manual cue adjustments necessary in some experiments.

During experimentation, the arm rest and haptic interface were visually occluded with a re-purposed face shield, with paper attached to the inside, worn on the side of the head to block visual feedback from the device. The subject wore headphones playing pink noise to mask any audible noise from the test bed that might influence their responses during the outlined psychophysical assessments.

The zero position (origin) of the end-effector within the workspace was found using a calibration procedure before each task (ASR or JND) was completed. To ensure good contact between the spherical end-effector and the skin, the origin was defined when the normal force read 0.5 N.

D. Maximum Comfort Threshold Protocol

Each participant will have a unique comfort threshold for the maximum displacement and force values that can be tolerated in the normal and shear directions. In this study, the method of adjustments was used to identify these upper limits. Though

less robust than other psychophysical tests, the participant's control of cue magnitudes in the method of adjustments protocol is well-suited to this experiment. Alternative psychophysical tests determine a threshold by delivering cues both greater than and less than the threshold magnitude, necessarily resulting in multiple cues uncomfortable to the participant. Since the method of adjustments allows the participant to regulate the cues, they are protected from experiencing cues beyond their comfort range.

First the normal direction was tested with a random initial displacement between 3.0 and 4.5 mm (position control), a range determined in pilot testing. From this initial value, the subject could adjust the cue to be larger or smaller until they reached what they deemed as their comfort limit. The comfort level was described to the subjects as the point where, "if this happened briefly, once in a while, it would be fine. More than this is not okay." After the subject confirmed their setting, the cue was then released to complete the trial. This process was repeated for a total of four trials.

The procedure was then repeated for cues in the shear direction. For these trials, the normal force was fixed at 70% of the maximum normal force value determined from the previous trials. This value of normal force was selected to be toward the upper end of the range to ensure a salient sensation with limited slip, while still preserving participant comfort over multiple trials.

E. Minimum Absolute Threshold Protocol

The staircase method was used to determine the absolute detection thresholds for cues that are provided in both the position-control and force-control modes of the test bed. These values are the smallest detectable cues that the user can perceive. The staircase method was used due to its time efficiency and due to our interest in finding the threshold without having to determine the full psychometric function [51], [55]. This threshold is unique to each participant, and was determined through a series of psychophysical comparisons between a zero stimulus to some comparison value, which was increased or decreased depending on the user's response. The initial comparison value was a random value between 10% and 15% of the corresponding maximum comfort threshold.

In each trial, the zero reference value and the comparison were presented to the participant in a randomized order, asking which is of greater magnitude. If the participant correctly identified that the comparison was larger in magnitude, the comparison value was decreased by a fixed increment of either 0.05 N (force) or 0.2 mm (position) in the next trial. If the participant's response was incorrect (selecting the zero reference stimulus as greater in magnitude), then the comparison stimulus was increased by the same fixed increment.

Successive trials with the same directional change, either increasing or decreasing the magnitude of the comparison cue, are called a run. The change from an increasing to decreasing run is referred to as a reversal. The trial was completed after twelve reversals, indicating the transition points between differentiating and not differentiating the comparison from the reference stimulus. This process was repeated for five trials in position control for both the normal and shear directions.

F. Mid-Range Just Noticeable Difference Protocol

In order to measure the perceptual resolution of a haptic sensation, the just noticeable difference (JND), or difference threshold, was used to quantify the required change of the stimulus to be differentiated against the original, or reference stimulus. The JND may vary across the full range of stimulus values. Despite this, comparing the JND at one specific stimulus magnitude across subjects will provide insight into the variation of haptic perception resolution among them. The Method of Constant Stimuli was used to quantify the JND, and was chosen since the method produces an entire psychometric curve, rather than just the JND threshold [51]. This allows us to have a clearer picture, and enables comparisons of the psychometric curve across subjects to determine the degree of agreement.

The JND was assessed for both normal and shear movements of the end effector, in both position control and force control schemes. The reference stimulus was chosen as 70% of the individual's ASR for both position control conditions and for the normal-force condition. The reference stimulus was chosen as 50% of the ASR for the shear-force condition to avoid instances of slipping between the end effector and the skin which occurred at some points in early experimentation. The choice of 70% is arbitrary, but was selected to be on the upper end of the ASR to be easily discernible, but not so high to exceed anyone's comfort threshold. During the experiment, the reference was compared against seven comparison values, centered at the reference value. In this case they were spaced at increments of 4% of the ASR for position or force, for the corresponding control scheme.

For each trial the reference and comparison were presented to the participant in a random order, pressing or stretching the skin by the predefined amount. Users reported which they perceived to be larger in magnitude, the first or second stimulus. This was repeated for each comparison-reference pair for a total of 20 trials per pair, for all seven pairs, presented in a randomized order for a total of 140 trials per normal/shear position/force condition. The four conditions were presented in two experimental sessions, one for each control mode (position or force). After each session, the participants completed a survey.

G. Likert Survey

To assess the subjects' perception of the cues, experiments, and their performance, subjects were asked to rate statements on a continuous scale from zero to ten, representing "Strongly Disagree" to "Strongly Agree" (see Table III).

V. Data Analysis

A. Maximum Comfort Threshold

The maximum comfort thresholds for the normal and shear DOFs in position control were determined by averaging the user responses across the four repeated trials in each condition. The maximum comfort thresholds to be used in force control were defined as the mean forces at the corresponding position thresholds in the normal and shear directions. The upper bound

for any commanded cue to a participant was capped at 80% of their maximum comfort threshold. Two upper bounds were computed, namely the force upper bound and the position upper bound.

B. Minimum Absolute Threshold Determination

The values of the last six reversals of each trial were averaged to define the absolute threshold in each trial. The force threshold was defined as the mean of the force values at the reversal positions, and calculated in the same manner.

C. Mid-Range Just Noticeable Difference Determination

Each comparison value was compared against the reference twenty times to ask which was larger, the proportion of correct responses for each comparison is plotted against its value. The points were fitted to a sigmoid function:

$$f(x) = \frac{1}{1 + e^{-x}} \tag{3}$$

Ideally the curve would be a step function, where the reference is identified as larger than any value lower than it and the comparison as larger for any value higher than the reference, though this is not the case in practical implementation as the difference between the reference and comparison values become closer in value. The sigmoid function is related to the cumulative distribution function representing the probability of choosing the comparison value as larger than the reference value as it varies within the range where there is any confusion. In a proper design, the reference is always identified as larger than the smallest comparison and is never identified as larger than the largest comparison. The proportion of comparing it against itself should be 50%. The just noticeable difference (JND) is then determined using the psychometric curve by calculating half the difference between the points where the comparison is chosen 25% of the time and 75% of the time:

$$JND = \frac{x_{75} - x_{25}}{2} \tag{4}$$

This defines the domain where the comparison can be differentiated from the reference at least 75% of the time. The JND is reported as a physical value, in either Newtons or millimeters. We also report the JND as a percentage of the ASR, which we define as the normalized JND. This allows us to see how these values provide an estimate for the number of distinct stimuli that can be detected within the ASR.

D. Statistical Analyses

T-tests were used to compare the relative number of distinct stimuli that comprise the ASR between position and force control, as determined by the normalized JND.

VI. Results

The psychophysical testing provides mechanisms for determining the participants' thresholds, either to tolerate (measured via the maximum threshold), to detect (measured via the absolute threshold), or to differentiate (measured via the just noticeable difference (JND) threshold), haptic cues applied to the arm in the normal and shear directions, under both position and force control modes of the test bed. Taken together, these thresholds provide a picture of how haptic experiences differ between people for various conditions and comprise our proposed metric, the Allowable Stimulus Range (ASR).

A. Psychophysical Thresholds

Threshold data are summarized in Table II, and the ASR and JND values are visualized in Fig. 5 for each DOF-controller combination. The bars represent the ASR, bounded by minimum and maximum values, and for clarity the minimum values are also plotted in Fig. 6. The JND is visualized as an error bar about its reference value, showing how much the reference cue value would need to change to be perceived by the participant as a different cue. The allowable position ranges for normal indentation vary from the absolute thresholds, ranging from 0.22 to 1.42 mm, to the maximum comfort thresholds, between 13.59 to 32.13 mm. Similarly, the force boundaries in normal indentation ranges vary from absolute thresholds between 0.38 to 0.96 N to maximum comfort thresholds in the 4.76 to 37.75 N range. Thresholds in the shear direction of skin stretch also have a wide distribution, ranging from 0.15 to 0.30 mm to between 13.9 and 45.92 mm for absolute and comfort thresholds in position control, and between -0.4 to 2.03 N and 1.82 to 24.84 N in force control.

In conceptualizing the JND as an increment to create a distinct cue from the reference, it can also then be normalized by the stimulus range in order to visualize what percentage of the ASR this covers (Fig. 7). Each JND is defined about a specific reference point, and it could vary for other possible reference values over the ASR. For example, the JND could be much larger before much stretch is applied, and it could be smaller toward the upper limit of the range, where the preload is significant. Regardless, if someone had a narrow ASR, but a large JND, then they would only be able to perceive differences between a small number of stimuli for that chosen haptic cue interaction. For normal indentation, the normalized JND ranges from 2-6% (3.5% $\pm$ 1.2) of the ASR for position control and 4-14% (7.9% $\pm$ 3.5) for force control. These ranges are significantly different ($p < .001$), showing as the ranges are currently defined, force control is less sensitive that position control. Under shear loading, the cues were applied at different points in their respective ASR, with a 70% reference for position control, and 50% for force control, so they aren't directly comparable. However, if the JND is assumed constant across the range of motion and they are compared, there is no statistical difference, with position JNDs ranging from 3-19% (6.8% $\pm$ 4.9) and force JNDs from 4-9% (5.5% $\pm$ 2.3).

B. Likert Survey

A Likert survey was administered to measure participant agreement with the statements listed in Table III using a continuous scale from zero to ten, where zero is strongly disagree, ten is strongly agree, and five is neutral. Overall participants found position control significantly more intuitive than force control, p = .03, d = 0.72. Though there are no

TABLE I
NORMAL STIMULUS THRESHOLD METRICS

	S1	S2	S3	S4	S5	S6	S7	S8	S9	S10	S11	S12	S13	S14	S15	S16
Absolute Thresholds - ASR Lower Bound																
Position [mm]	0.30	0.26	0.27	0.31	0.25	0.24	0.30	0.31	0.24	0.28	0.24	1.42	0.22	0.26	0.24	-
Force [N]	0.56	0.55	0.71	0.38	0.68	0.59	0.51	0.63	0.52	0.72	0.59	0.96	0.40	0.60	0.49	-
Comfort Thresholds - ASR Upper Bound																
Position [mm]	23.08	17.42	18.01	24.10	13.59	13.47	25.40	14.68	19.71	15.82	16.37	19.84	24.83	32.13	28.39	29.78
Force [N]	25.12	10.08	11.78	18.78	4.89	10.99	23.00	5.38	15.94	7.15	4.76	10.81	22.12	35.40	37.75	32.51
Allowable Stimulus Range Size																
Position [mm]	22.78	17.16	17.74	23.80	13.34	13.23	25.10	14.37	19.46	15.55	16.13	18.43	24.60	31.87	28.14	29.78
Force [N]	24.56	9.53	11.07	18.41	4.21	10.40	22.49	4.75	15.42	6.43	4.17	9.86	21.72	34.81	37.26	32.51
JND Thresholds																
Position Ref. [mm]	16.26	12.16	12.66	17.07	9.48	9.55	17.75	10.24	13.73	11.02	11.30	-	17.33	22.41	19.85	20.77
% Range [-]	0.70	0.69	0.70	0.70	0.69	0.70	0.70	0.69	0.69	0.69	0.69	-	0.70	0.70	0.70	0.70
Increment [mm]	0.80	0.62	0.62	0.82	0.48	0.45	0.90	0.52	0.70	0.56	0.60	-	0.88	1.14	1.00	1.06
Position JND [mm]	0.66	0.42	0.76	0.65	0.80	0.24	1.06	0.80	0.80	0.50	0.55	-	1.00	0.80	0.65	1.02
Normalized JND [-]	0.03	0.02	0.04	0.03	0.06	0.02	0.04	0.06	0.04	0.03	0.03	-	0.04	0.02	0.02	0.03
Force Ref. [N]	17.50	7.10	-	13.11	3.62	7.78	16.00	3.85	11.13	5.12	-	7.71	15.38	24.60	26.18	22.61
% Range [-]	0.69	0.69	-	0.69	0.70	0.69	0.69	0.68	0.69	0.68	-	0.68	0.69	0.69	0.69	0.70
Increment [N]	0.90	0.35	-	0.67	0.16	0.37	0.83	0.17	0.56	0.23	-	0.36	0.80	1.27	1.37	1.17
Force JND [N]	0.94	0.45	-	1.37	0.59	0.74	2.29	0.59	1.74	0.47	-	1.24	0.99	1.58	1.40	2.27
Normalized JND [-]	0.04	0.05	-	0.07	0.14	0.07	0.10	0.12	0.11	0.07	-	0.13	0.05	0.05	0.04	0.07

TABLE II
SHEAR STIMULUS THRESHOLD METRICS

Questions	S1	S2	S3	S4	S5	S6	S7	S8	S9	S10	S11	S12	S13	S14	S15	S16
Absolute Thresholds - ASR Lower Bound																
Position [mm]	0.23	0.20	0.29	0.24	0.19	0.21	0.15	0.17	0.18	0.19	0.18	0.18	0.17	0.21	0.22	0.30
Force [N]	-0.27	0.11	-0.12	-0.08	-0.20	-0.17	0.17	-0.01	0.15	0.04	-0.08	0.02	-0.40	0.69	2.03	0.65
Comfort Thresholds - ASR Upper Bound																
Position [mm]	22.88	22.95	18.74	32.08	20.72	20.03	13.90	20.63	20.08	34.23	18.71	29.03	45.92	45.54	45.63	41.73
Force [N]	3.08	5.70	3.11	5.14	1.82	3.02	2.90	2.08	3.24	6.16	2.34	4.68	11.23	12.24	24.84	14.41
Allowable Stimulus Range Size																
Position [mm]	22.66	22.76	18.45	31.84	20.54	19.82	13.75	20.46	19.91	34.04	18.53	28.85	45.75	45.32	45.41	41.43
Force [N]	3.35	5.60	3.24	5.22	2.01	3.18	2.73	2.09	3.08	6.12	2.42	4.66	11.63	11.55	22.81	13.76
JND Thresholds																
Position Ref. [mm]	-	16.02	13.15	22.37	14.43	13.93	9.64	14.23	13.86	23.62	13.03	-	32.08	31.84	31.48	29.11
% Range [-]	-	0.70	0.70	0.69	0.69	0.69	0.69	0.69	0.69	0.69	0.69	-	0.70	0.70	0.69	0.70
Increment [mm]	-	0.81	0.65	1.14	0.74	0.72	0.50	0.76	0.74	1.26	0.67	-	1.63	1.61	1.68	1.48
Position JND [mm]	-	0.66	0.96	2.00	1.49	0.70	2.16	1.47	3.82	1.01	1.45	-	1.36	1.54	1.89	2.81
Normalized JND	-	0.03	0.05	0.06	0.07	0.04	0.16	0.07	0.19	0.03	0.08	-	0.03	0.03	0.04	0.07
Force Ref. [N]	1.42	2.76	1.52	2.41	0.92	1.45	-	-	1.49	2.83	-	-	5.17	6.25	-	-
% Range [-]	0.51	0.47	0.51	0.48	0.55	0.51	-	-	0.43	0.46	-	-	0.48	0.48	-	-
Increment [N]	0.11	0.20	0.11	0.19	0.06	0.11	-	-	0.12	0.23	-	-	0.41	0.40	-	-
Force JND [N]	0.12	0.45	0.15	0.40	0.16	0.12	-	-	0.28	0.20	-	-	0.37	0.46	-	-
Normalized JND	0.04	0.08	0.05	0.08	0.08	0.04	-	-	0.09	0.03	-	-	0.03	0.04	-	-

other statistically significant effects, the effect sizes suggest that under force control, the cues were more pleasant, although they were perceived as more similar to each other. Beyond this, the participants were well insulated from environmental noise.

VII. DISCUSSION

Three main contributions are presented in this paper: the definition of the *allowable stimulus range* (ASR) and methods for its determination, a new haptic test bed for tangential skin stretch and normal indentation cues on the arm in either closed-loop position or force control operation modes, and a comparison of the ASR under the two control schemes to determine if one control scheme is more advantageous.

A. Allowable Stimulus Range

In order to define a safe and effective cue region for each individual, we define the ASR using results of standard psychophysical experiments. We determined the minimum stimuli that participants can detect, the maximum cue amplitude they could tolerate, as well as the amount that a cue should change to be recognizable as different than a reference. These are determined using the absolute, maximum comfort, and just noticeable difference (JND) thresholds. The absolute thresholds ranged considerably between participants, with the highest participant threshold two to six times the lowest value in each DOF-controller condition. This experience corroborates participant feedback from previous experiments, where subjects given the same conditions reported varying degrees of comfort and perceptibly [23]. The definition of the ASR provides a means of defining the safe operating region of a haptic cue. Each individual will have a unique ASR for each cue type and each controller, able to be ascertained in fifteen to twenty minutes, providing a method of customizing haptic devices and cues to each user.

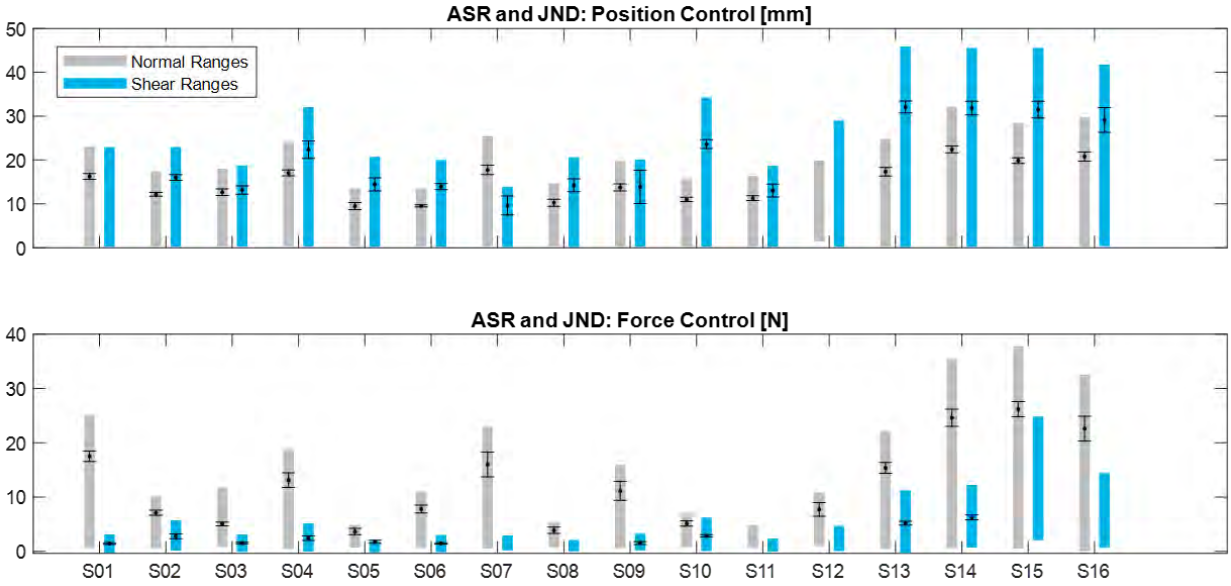

Fig. 5. ASR and JND for each participant for each of the four controller-DOF conditions. ASR is illustrated with shaded bars, and spans from the absolute threshold to the comfort threshold. The reference value for the JND is overlaid on each ASR, showing the JND at that reference as an error bar.

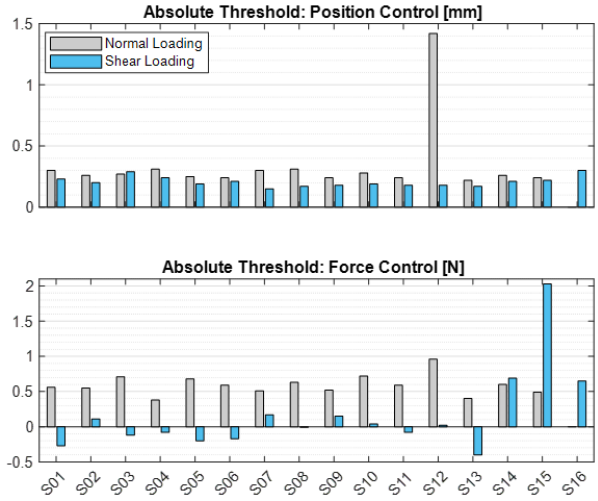

Fig. 6. Absolute detection thresholds for each loading condition and participant are reported as displacements in mm for the position control scheme, and as forces in N for the force control scheme.

TABLE III
LIKERT RESPONSES: POSITION AND FORCE CONTROL

Questions	Position Control Mean (Std.)	Force Control Mean (Std.)	p-value	Cohen's d
Clarity				
Interacting with the device was intuitive	6.14 (2.75)	3.64 (2.85)	0.03	0.72
I was confused about how to interpret the device	5.53 (3.31)	6.78 (1.73)	0.24	0.36
It was easy to distinguish between haptic sensations	6.02 (2.83)	4.61 (2.53)	0.13	0.47
The haptic sensations displayed felt similar to one another	5.53 (3.03)	7.07 (2.03)	0.09	0.53
The cues became clearer over the course of the test	4.71 (2.32)	4.64 (3.12)	0.94	0.02
I had a had more difficulty feeling cues later in the test	5.07 (3.04)	6.45 (2.06)	0.30	0.31
I am confident in my responses during this test	5.95 (3.02)	5.73 (2.99)	0.88	0.05
I had difficulty responding in this test	5.75 (3.13)	4.95 (2.31)	0.36	0.27
Quality				
The sensations from the system felt pleasant	4.02 (2.68)	6.34 (2.50)	0.07	0.58
The sensations from the system were unpleasant	6.94 (2.01)	4.68 (2.53)	0.06	0.62
I would have been happy to continue the experiment for longer	5.01 (2.17)	4.65 (2.34)	0.70	0.11
At the end of the experiments I felt tired	6.02 (2.87)	6.16 (2.15)	0.86	0.05
I was comfortable when using this device	3.83 (2.68)	6.30 (2.48)	0.06	0.60
I found the device uncomfortable	4.52 (2.42)	6.58 (3.28)	0.11	0.50
Environment				
I was well insulated from outside noise during this test	4.69 (2.19)	4.80 (2.62)	0.92	0.03
I was often distracted during this test	5.92 (2.48)	3.50 (3.03)	0.13	0.47

There are opportunities for further exploration into the ASR definition for frictional interfaces, specifically related to the velocity of the cues. We know that cue application velocity does not significantly impact the JND [18]; however, it may influence the frictional contact between the end-effector and the skin. For a few subjects, we observed negative absolute thresholds in the shear-force condition. This result would be expected under position control if there was slip at the contact interface, because when the end effector returns to the origin, it will stretch the skin the opposite way causing a negative force reading. The absolute threshold experiments were conducted under position control, and the force threshold is taken to be the force reading at the position threshold. Similarly for the JND experiments, the shear-force JND reference was decreased from 75% to 50% of the ASR to avoid slip. The reference value is then defined by the maximum comfort threshold. The JND experiments were conducted at a fast speed, whereas the maximum comfort threshold experiments were participant controlled, at a much slower velocity as they approached their maximum comfort threshold. The frictional interface and its design requirements are certainly an important topic of further research, and would not only be impacted by cue actuation speed, but by other factors such as humidity, perspiration, or the end effector material characteristics.

B. High-fidelity Test Bed

The psychophysical test bed presented in this paper is designed for detailed studies of human perception of haptic

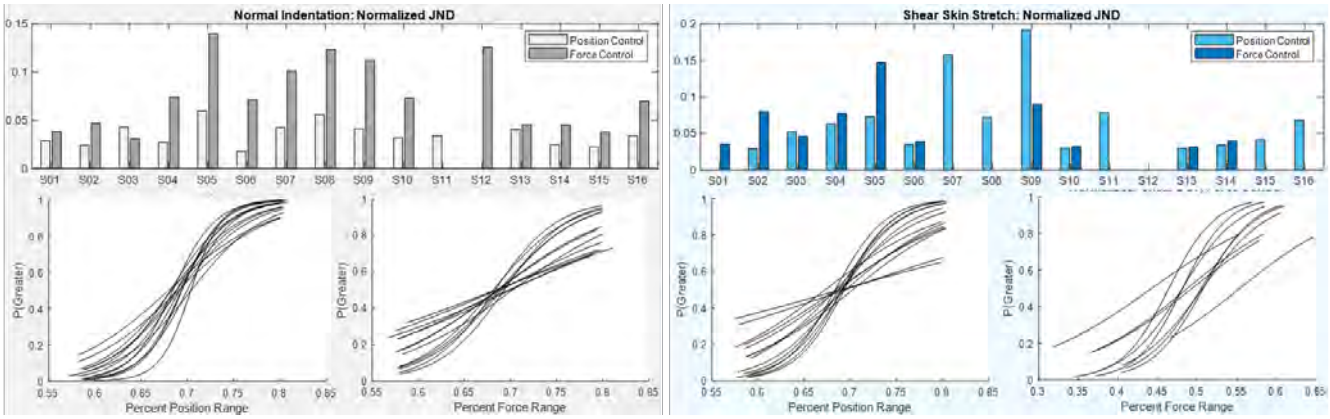

Fig. 7. Normalized JNDs for each of the four controller-DOF conditions, as a percentage of the ASR to show the maximum number of discrete cues that might be perceivable within a participant's ASR, assuming that the JND is constant over the ASR.

stimuli, measuring the force-torque interactions between the end-effector for both normal and shear displacements of the skin. The material that comprises the interface between the end-effector and the skin is comparable to materials used in state of the art wearable haptic devices. The design is modular, allowing for the end-effector to be replaced with other materials or geometries as a given study requires. The adjustable design of the arm rest can easily be fitted to people of varying arm sizes, as well as testing perception of cues applied to different locations and orientations on the arm.

The software developed to control the device is modular, allowing for seamless transitions between control schemes, both the position and force control represented here as well as the ability to insert new controller options. The data acquisition interface and code base also allow for easy access to key measurement and control values and parameters.

Two controllers were developed for the experiments presented here, a classic PD position controller and an adapted PD force controller, using velocity rather than a force derivative term. These two controllers provide the opportunity to compare control schemes when measuring the haptic perception of skin stretch and indentation cues. The perceptual performance of some subjects surpassed our expectations, with most absolute thresholds on the same order of magnitude as the measurement precision of the test bed, 0.25 mm. This was unexpected, with subjects able to perceive much smaller cues than we anticipated based on pilot testing. In future studies this should be investigated and rectified in the test bed design.

C. Effect of Position vs. Force Control on Perception

Typically, wearable haptic devices employ a position control scheme to realize the haptic cue, with large variability in cue perception observed between individuals [23]. Noting the differences in people's physiological make-up of muscle and fat, we hypothesized that these differences result in different forces applied to the skin for the same displacement, and force control would provide a haptic experience more adapted to their physiology. We hypothesized the force domain would result in more consistent psychophysical thresholds between subjects. If the JNDs determined when cues are provided using force control are normalized by the allowable stimulus range, they range from 4 to 14% for normal indentation and 4 to 9% for skin stretch. For some users, this is a substantial percentage of their allowable stimulus range. The results of these experiments demonstrate the high tactile acuity in some individuals and the limitations in the level of detail that exist in haptic perception for skin stretch and indentation in others.

Using a force control scheme to provide haptic cues did not result in more consistent perceptual thresholds across participants compared to a position control scheme. Therefore, it is not enough to ensure that the forces perceived by the user during normal indentation and skin stretch are consistent in order to achieve consistent haptic experiences. At least in using either position or force controllers, some degree of adjustments are necessary to optimize a device to a specific individual. Further investigation into the unique participant physiology and contact mechanics during the haptic cue interactions will provide further insight into the extent that the physical interactions impact haptic perception.

Normalization of JNDs, in addition to providing insight into tactile acuity, allows us to compare acuity across control schemes. In comparing the JNDs under two control schemes for normal indentation, cues under position control have smaller normalized JNDs compared to those under force control, showing position control as more effective for creating more distinct cues.

When comparing the two control schemes based on subject impressions, the Likert surveys show position control is in fact more intuitive than force control, again differing from our hypothesis that force control would be a more effective haptic control scheme. The effect sizes do imply however that the cues conveyed via force control were felt as more comfortable than those delivered with position control. Further investigation into the characteristics of the cue, such as smoothness and magnitude of force and displacement, would be interesting to assess in order to clarify this point.

VIII. Conclusion

In order to increase the salience and efficacy of wearable haptic devices, it is becoming evident that the ranges and

preferred magnitudes of haptic cues vary between users. This work explores this topic in two ways, first by defining and measuring the *allowable stimulus range* (ASR), defined for each cue and unique user and bounded by the minimum detectable cue size and the maximum comfortable magnitude. The second avenue of investigation is by comparing the haptic perception metrics under position and force control, with the hypothesis that a force control method can provide the necessary adjustments to user physiology. The third contribution of this work is the presentation of a custom test bed that is able to precisely provide normal indentation and skin stretch haptic cues. The testbed developed to complete psychophysical experiments and measure the ASR was designed to be a flexible experimental platform. The software included two controllers, position control and force control, as well as three psychophysical tests, method of adjustments, method of constant stimuli, and the staircase method. The hardware provides fully instrumented indentation and shear haptic cues, and features a modular armrest to adjust the hardware to be comfortable to individual users at several orientations and places on the arm. The three psychophysical assessments demonstrate the wide variability in perceptible, comfortable, and distinguishable thresholds between individuals, visualized by the size and inclusive values in the ASR measurements. The experiments show for the chosen cues in indentation and skin stretch, position control is more intuitive and has higher perceptual resolution, though effect sizes indicate force control, while harder to distinguish, as more comfortable way to receive haptic cues. The data confirm the large variability in perceptual acuity between people, but also variability for each person through changes in control scheme and DOF. Since the same variability between ASRs and JNDs occur in both control schemes, the change in controller is not sufficient to accommodate preferences of users, and some time to determine their ASR for that cue is necessary to provide a comfortable and effective haptic cue range for each user. In order to delve deeper into the mechanisms behind differences in tactile acuity between individuals, we should consider the variability in the physical make-up of those individuals, and the changes in haptic interface with varying environmental conditions, activity level, and device actuation speed.

ACKNOWLEDGMENT

The authors would like to thank Dr. Evan Pezent, Dr. Nathan Dunkelberger, Dr. Zane Zook, Doris Xu, and Lisa Zhu for their support on this project.

REFERENCES

[1] C. Antfolk, M. D'alonzo, B. Rosén, G. Lundborg, F. Sebelius, and C. Cipriani, "Sensory feedback in upper limb prosthetics," *Expert review of medical devices*, vol. 10, no. 1, pp. 45–54, 2013.

[2] E. Battaglia, J. P. Clark, M. Bianchi, M. G. Catalano, A. Bicchi, and M. K. O'Malley, "Skin stretch haptic feedback to convey closure information in anthropomorphic, under-actuated upper limb soft prostheses," *IEEE transactions on haptics*, vol. 12, no. 4, pp. 508–520, 2019.

[3] J. P. Clark, G. Lentini, F. Barontini, M. G. Catalano, M. Bianchi, and M. K. O'Malley, "On the role of wearable haptics for force feedback in teleimpedance control for dual-arm robotic teleoperation," in *2019 International Conference on Robotics and Automation (ICRA)*, pp. 5187–5193, IEEE, 2019.

[4] D. Wang, K. Ohnishi, and W. Xu, "Multimodal haptic display for virtual reality: A survey," *IEEE Transactions on Industrial Electronics*, vol. 67, no. 1, pp. 610–623, 2019.

[5] J. D. Brown, T. S. Kunz, D. Gardner, M. K. Shelley, A. J. Davis, and R. B. Gillespie, "An empirical evaluation of force feedback in body-powered prostheses," *IEEE Transactions on Neural Systems and Rehabilitation Engineering*, vol. 25, no. 3, pp. 215–226, 2016.

[6] G. R. VandenBos, *APA dictionary of psychology.* American Psychological Association, 2007.

[7] K. T. Yoshida, C. M. Nunez, S. R. Williams, A. M. Okamura, and M. Luo, "3-dof wearable, pneumatic haptic device to deliver normal, shear, vibration, and torsion feedback," in *2019 IEEE World Haptics Conference (WHC)*, pp. 97–102, IEEE, 2019.

[8] H. Culbertson, C. M. Nunez, A. Israr, F. Lau, F. Abnousi, and A. M. Okamura, "A social haptic device to create continuous lateral motion using sequential normal indentation," in *2018 IEEE Haptics Symposium (HAPTICS)*, pp. 32–39, IEEE, 2018.

[9] R. Omori, Y. Kuroda, S. Yoshimoto, and O. Oshiro, "A wearable skin stretch device for lower limbs: investigation of curvature effect on slip," in *2019 IEEE World Haptics Conference (WHC)*, pp. 37–42, IEEE, 2019.

[10] C. Antfolk, A. Björkman, S.-O. Frank, F. Sebelius, G. Lundborg, and B. Rosen, "Sensory feedback from a prosthetic hand based on air-mediated pressure from the hand to the forearm skin," *Journal of rehabilitation medicine*, vol. 44, no. 8, pp. 702–707, 2012.

[11] L. H. Kim, P. Castillo, S. Follmer, and A. Israr, "Vps tactile display: Tactile information transfer of vibration, pressure, and shear," *Proceedings of the ACM on Interactive, Mobile, Wearable and Ubiquitous Technologies*, vol. 3, no. 2, pp. 1–17, 2019.

[12] N. Agharese, T. Cloyd, L. H. Blumenschein, M. Raitor, E. W. Hawkes, H. Culbertson, and A. M. Okamura, "Hapwrap: Soft growing wearable haptic device," in *2018 IEEE International Conference on Robotics and Automation (ICRA)*, pp. 5466–5472, IEEE, 2018.

[13] E. Battaglia, J. P. Clark, M. Bianchi, M. G. Catalano, A. Bicchi, and M. K. O'Malley, "The rice haptic rocker: skin stretch haptic feedback with the pisa/iit softhand," in *2017 IEEE World Haptics Conference (WHC)*, pp. 7–12, IEEE, 2017.

[14] N. A. Caswell, R. T. Yardley, M. N. Montandon, and W. R. Provancher, "Design of a forearm-mounted directional skin stretch device," in *2012 IEEE Haptics Symposium (HAPTICS)*, pp. 365–370, IEEE, 2012.

[15] D. K. Chen, I. A. Anderson, C. G. Walker, and T. F. Besier, "Lower extremity lateral skin stretch perception for haptic feedback," *IEEE transactions on haptics*, vol. 9, no. 1, pp. 62–68, 2016.

[16] C. Wang, D.-Y. Huang, S.-w. Hsu, C.-E. Hou, Y.-L. Chiu, R.-C. Chang, J.-Y. Lo, and B.-Y. Chen, "Masque: Exploring lateral skin stretch feedback on the face with head-mounted displays," in *Proceedings of the 32nd Annual ACM Symposium on User Interface Software and Technology*, pp. 439–451, 2019.

[17] A. Haynes, M. F. Simons, T. Helps, Y. Nakamura, and J. Rossiter, "A wearable skin-stretching tactile interface for human–robot and human–human communication," *IEEE Robotics and Automation Letters*, vol. 4, no. 2, pp. 1641–1646, 2019.

[18] S. Y. Kim, J. P. Clark, P. Kortum, and M. K. O'Malley, "The influence of cue presentation velocity on skin stretch perception," in *2019 IEEE World Haptics Conference (WHC)*, pp. 485–490, IEEE, 2019.

[19] M. Zhu, A. H. Memar, A. Gupta, M. Samad, P. Agarwal, Y. Visell, S. J. Keller, and N. Colonnese, "Pneusleeve: In-fabric multimodal actuation and sensing in a soft, compact, and expressive haptic sleeve," in *Proceedings of the 2020 CHI Conference on Human Factors in Computing Systems*, pp. 1–12, 2020.

[20] J. J. Fleck, Z. A. Zook, T. W. Tjandra, and M. K. O'Malley, "A cutaneous haptic cue characterization testbed," in *2019 IEEE World Haptics Conference (WHC)*, pp. 319–324, IEEE, 2019.

[21] N. A.-h. Hamdan, A. Wagner, S. Voelker, J. Steimle, and J. Borchers, "Springlets: Expressive, flexible and silent on-skin tactile interfaces," in *Proceedings of the 2019 CHI Conference on Human Factors in Computing Systems*, pp. 1–14, 2019.

[22] L. Meli, I. Hussain, M. Aurilio, M. Malvezzi, M. K. O'Malley, and D. Prattichizzo, "The hbracelet: a wearable haptic device for the distributed mechanotactile stimulation of the upper limb," *IEEE Robotics and Automation Letters*, vol. 3, no. 3, pp. 2198–2205, 2018.

[23] J. P. Clark, S. Y. Kim, and M. K. O'Malley, "The rice haptic rocker: Altering the perception of skin stretch through mapping and geometric design," in *2018 IEEE Haptics Symposium (HAPTICS)*, pp. 192–197, IEEE, 2018.

[24] K. Bark, J. Wheeler, P. Shull, J. Savall, and M. Cutkosky, "Rotational skin stretch feedback: A wearable haptic display for motion," *IEEE Transactions on Haptics*, vol. 3, no. 3, pp. 166–176, 2010.

[25] K. Kim, J. E. Colgate, J. J. Santos-Munné, A. Makhlin, and M. A. Peshkin, "On the design of miniature haptic devices for upper extremity prosthetics," *IEEE/ASME Transactions On Mechatronics*, vol. 15, no. 1, pp. 27–39, 2009.
[26] M. R. Motamedi, D. Florant, and V. Duchaine, "comparing the exteroceptive feedback of normal stress, skin stretch, and vibrotactile stimulation for restitution of static events," *Frontiers in Robotics and AI*, vol. 4, p. 6, 2017.
[27] D. Sierra González and C. Castellini, "A realistic implementation of ultrasound imaging as a human-machine interface for upper-limb amputees," *Frontiers in neurorobotics*, vol. 7, p. 17, 2013.
[28] K.-U. Kyung, J. Lee, and J.-S. Park, "Pen-like haptic interface and its application on touch screen," in *RO-MAN 2007-The 16th IEEE International Symposium on Robot and Human Interactive Communication*, pp. 9–13, IEEE, 2007.
[29] B. Stephens-Fripp, R. Mutlu, and G. Alici, "Applying mechanical pressure and skin stretch simultaneously for sensory feedback in prosthetic hands," in *2018 7th IEEE International Conference on Biomedical Robotics and Biomechatronics (Biorob)*, pp. 230–235, IEEE, 2018.
[30] E. Pezent, P. Agarwal, J. Hartcher-O'Brien, N. Colonnese, and M. K. O'Malley, "Design, control, and psychophysics of tasbi: A force-controlled multimodal haptic bracelet," *IEEE Transactions on Robotics*, vol. 38, no. 5, pp. 2962–2978, 2022.
[31] P. T. Burgess and E. Perl, "Cutaneous mechanoreceptors and nociceptors," in *Somatosensory system*, pp. 29–78, Springer, 1973.
[32] F. Chinello, C. Pacchierotti, N. G. Tsagarakis, and D. Prattichizzo, "Design of a wearable skin stretch cutaneous device for the upper limb," in *2016 IEEE Haptics Symposium (HAPTICS)*, pp. 14–20, IEEE, 2016.
[33] J. L. Sullivan, N. Dunkelberger, J. Bradley, J. Young, A. Israr, F. Lau, K. Klumb, F. Abnousi, and M. K. O'Malley, "Multi-sensory stimuli improve distinguishability of cutaneous haptic cues," *IEEE Transactions on Haptics*, vol. 13, no. 2, pp. 286–297, 2019.
[34] H. Choi, B. Son, S. Kim, Y. Oh, and J. Park, "A wearable hand haptic interface to provide skin stretch feedback to the dorsum of a hand," in *International AsiaHaptics conference*, pp. 205–209, Springer, 2018.
[35] J.-B. Chossat, D. K. Chen, Y.-L. Park, and P. B. Shull, "Soft wearable skin-stretch device for haptic feedback using twisted and coiled polymer actuators," *IEEE transactions on haptics*, vol. 12, no. 4, pp. 521–532, 2019.
[36] A. Akhtar, M. Nguyen, L. Wan, B. Boyce, P. Slade, and T. Bretl, "Passive mechanical skin stretch for multiple degree-of-freedom proprioception in a hand prosthesis," in *International Conference on Human Haptic Sensing and Touch Enabled Computer Applications*, pp. 120–128, Springer, 2014.
[37] A. Guzererler, W. R. Provancher, and C. Basdogan, "Perception of skin stretch applied to palm: Effects of speed and displacement," in *International Conference on Human Haptic Sensing and Touch Enabled Computer Applications*, pp. 180–189, Springer, 2016.
[38] S. Casini, M. Morvidoni, M. Bianchi, M. Catalano, G. Grioli, and A. Bicchi, "Design and realization of the cuff-clenching upper-limb force feedback wearable device for distributed mechano-tactile stimulation of normal and tangential skin forces," in *2015 IEEE/RSJ International Conference on Intelligent Robots and Systems (IROS)*, pp. 1186–1193, IEEE, 2015.
[39] C. Antfolk, C. Balkenius, G. Lundborg, B. Rosén, and F. Sebelius, "A tactile display system for hand prostheses to discriminate pressure and individual finger localization," *J Med Biol Eng*, vol. 30, no. 6, pp. 355–60, 2010.
[40] D. K. Chen, J.-B. Chossat, and P. B. Shull, "Haptivec: Presenting haptic feedback vectors in handheld controllers using embedded tactile pin arrays," in *Proceedings of the 2019 CHI Conference on Human Factors in Computing Systems*, pp. 1–11, 2019.
[41] K. Kim and J. E. Colgate, "Haptic feedback enhances grip force control of semg-controlled prosthetic hands in targeted reinnervation amputees," *IEEE Transactions on Neural Systems and Rehabilitation Engineering*, vol. 20, no. 6, pp. 798–805, 2012.
[42] A. Erwin and F. C. Sup IV, "A haptic feedback scheme to accurately position a virtual wrist prosthesis using a three-node tactor array," *PloS one*, vol. 10, no. 8, p. e0134095, 2015.
[44] N. Dunkelberger, J. L. Sullivan, J. Bradley, I. Manickam, G. Dasarathy, R. Baraniuk, and M. K. O'Malley, "A multisensory approach to present phonemes as language through a wearable haptic device," *IEEE Transactions on Haptics*, vol. 14, no. 1, pp. 188–199, 2020.
[43] M. Aggravi, F. Pausé, P. R. Giordano, and C. Pacchierotti, "Design and evaluation of a wearable haptic device for skin stretch, pressure, and vibrotactile stimuli," *IEEE Robotics and Automation Letters*, vol. 3, no. 3, pp. 2166–2173, 2018.
[45] Z. A. Zook, J. J. Fleck, and M. K. O'Malley, "Effect of tactile masking on multi-sensory haptic perception," *IEEE Transactions on Haptics*, vol. 15, no. 1, pp. 212–221, 2022.
[46] N. Dunkelberger, J. L. Sullivan, J. Bradley, I. Manickam, G. Dasarathy, R. Baraniuk, and M. K. O'Malley, "A multisensory approach to present phonemes as language through a wearable haptic device," *IEEE Transactions on Haptics*, vol. 14, no. 1, pp. 188–199, 2021.
[47] F. Chinello, C. Pacchierotti, J. Bimbo, N. G. Tsagarakis, and D. Prattichizzo, "Design and evaluation of a wearable skin stretch device for haptic guidance," *IEEE Robotics and Automation Letters*, vol. 3, no. 1, pp. 524–531, 2017.
[48] K. Bark, J. W. Wheeler, S. Premakumar, and M. R. Cutkosky, "Comparison of skin stretch and vibrotactile stimulation for feedback of proprioceptive information," in *2008 Symposium on haptic interfaces for virtual environment and teleoperator systems*, pp. 71–78, IEEE, 2008.
[49] F. E. Van Beek, R. J. King, C. Brown, M. Di Luca, and S. Keller, "Static weight perception through skin stretch and kinesthetic information: detection thresholds, jnds, and pses," *IEEE Transactions on Haptics*, vol. 14, no. 1, pp. 20–31, 2020.
[50] F. Chinello, M. Malvezzi, C. Pacchierotti, and D. Prattichizzo, "A three dofs wearable tactile display for exploration and manipulation of virtual objects," in *2012 IEEE Haptics Symposium (HAPTICS)*, pp. 71–76, IEEE, 2012.
[51] G. A. Gescheider, *Psychophysics: the fundamentals*. Psychology Press, 2013.
[52] K. Bark, J. Wheeler, G. Lee, J. Savall, and M. Cutkosky, "A wearable skin stretch device for haptic feedback," in *World Haptics 2009-Third Joint EuroHaptics conference and Symposium on Haptic Interfaces for Virtual Environment and Teleoperator Systems*, pp. 464–469, IEEE, 2009.
[53] J. P. Clark, S. Y. Kim, and M. K. O'Malley, "The rice haptic rocker: Comparing longitudinal and lateral upper-limb skin stretch perception," in *International Conference on Human Haptic Sensing and Touch Enabled Computer Applications*, pp. 125–134, Springer, 2018.
[54] C. D. Fryar, Q. Gu, C. L. Ogden, and K. M. Flegal, "Anthropometric reference data for children and adults; united states, 2011-2014," 2016.
[55] T. N. Cornsweet, "The staircase-method in psychophysics," *The American journal of psychology*, vol. 75, no. 3, pp. 485–491, 1962.

Janelle P. Clark received her A.S. in Engineering Science at Monroe Community College in 2012, her B.S. degree in Mechanical Engineering at Clarkson University in 2015, and her M.S. and Ph.D. in Mechanical Engineering at Rice University, Houston, TX, USA in 2017 and 2022, respectively. She is currently a postdoctoral researcher in the Human-Robot Interaction Laboratory in the Computer Science Department at the University of Massachusetts Lowell.

Marcia K. O'Malley (F '20) received the B.S. degree from Purdue University, West Lafayette, IN, USA, in 1996, and the M.S. and Ph.D. degrees from Vanderbilt University, Nashville, TN, USA, in 1999 and 2001, respectively, all in mechanical engineering. She is the Thomas Michael Panos Family Professor in mechanical engineering, in computer science, and in electrical and computer engineering with Rice University, Houston, TX, USA, and directs the Mechatronics and Haptic Interfaces Laboratory.